

χ_{c1} and χ_{c2} polarization as a probe of color octet channel

S.P. Baranov¹, A.V. Lipatov^{2,3}

April 8, 2020

¹*P.N. Lebedev Institute of Physics, Moscow 119991, Russia*

²*Skobeltsyn Institute of Nuclear Physics, Lomonosov Moscow State University, Moscow 119991, Russia*

³*Joint Institute for Nuclear Research, Dubna 141980, Moscow Region, Russia*

Abstract

We analyze the first LHC data on χ_{c1} and χ_{c2} polarization obtained very recently by the CMS Collaboration at $\sqrt{s} = 8$ TeV. We describe the perturbative production of $c\bar{c}$ pair with k_T -factorization approach and use nonrelativistic QCD formalism for the formation of bound states. We demonstrate that the polar anisotropy of χ_{c1} and χ_{c2} mesons is strongly sensitive to the color octet contributions. We extract the long-distance matrix elements for χ_{c1} and χ_{c2} mesons from the first CMS polarization measurement together with available LHC data on the χ_{c1} and χ_{c2} transverse momentum distributions (and their ratios) collected at $\sqrt{s} = 7$ TeV. Our fit points to unequal color singlet wave functions of χ_{c1} and χ_{c2} states.

PACS number(s): 12.38.-t, 13.20.Gd, 14.40.Pq

Very recently, the CMS Collaboration reported on the first measurement [1] of the polarization of prompt χ_{c1} and χ_{c2} mesons produced in pp collisions at the energy $\sqrt{s} = 8$ TeV. The polarizations were measured in the decay J/ψ helicity frame through the analysis of the χ_{c2} to χ_{c1} yield ratio as a function of the positive muon polar or azimuthal angle in the cascade $\chi_{cJ} \rightarrow J/\psi(\rightarrow \mu^+\mu^-) + \gamma$ in three bins of J/ψ transverse momentum. No difference has been seen between the χ_{c1} and χ_{c2} states in the azimuthal distributions, whereas they were observed to have significantly different polar anisotropies. Thus, at least one of these mesons should be strongly polarized along the helicity axis [1]. This result contrasts with the unpolarized scenario observed for direct S -wave charmonia (J/ψ , ψ') and bottomonia $\Upsilon(nS)$ at the LHC over a wide transverse momentum range (see, for example, [2, 3] and references therein).

A commonly accepted framework for the description of heavy quarkonia production and decay is the non-relativistic Quantum Chromodynamic (NRQCD) [4, 5]. The perturbatively calculated cross sections for the short distance production of a heavy quark pair $Q\bar{Q}$ in an intermediate state ${}^{2S+1}L_J^{(a)}$ with spin S , orbital angular momentum L , total angular momentum J , and color representation a are accompanied with long distance matrix elements (LDMEs) which describe the non-perturbative transition of intermediate $Q\bar{Q}$ pair into a physical meson via soft gluon radiation. The NRQCD calculations at next-to-leading order (NLO) successfully describe charmonia J/ψ , ψ' , χ_{cJ} [6–13] and bottomonia $\Upsilon(nS)$, $\chi_{bJ}(mP)$ [14–18] transverse momenta distributions and agree well with the first CMS data [1] on the χ_{cJ} polarization at the LHC. However, NRQCD has a long-standing challenge in the S -wave charmonia polarization (see, for example, discussions [19–21] and references therein). The description of η_c production data [22] reported recently by the LHCb Collaboration also turned out to be rather puzzling [23, 24]. So, at present the overall situation is still far from through understanding, and further theoretical studies are still an urgent task.

One possible solution has been proposed in [25]. This solution implies certain modification of the NRQCD rules. Usually, the final state gluons changing the color and other quantum numbers of quark pair and bringing it to the observed color singlet (CS) state are regarded as carrying no energy-momentum. This is in obvious contradiction with confinement which prohibits the emission of infinitely soft colored quanta. In reality, the heavy quark system must undergo a kind of final state interaction where the energy-momentum exchange must be larger than at least the typical confinement scale. Then, the classical multipole radiation theory can be applied to describe nonperturbative transformations of the color octet (CO) quark pairs produced in hard subprocesses into observed final state quarkonia. In this way, the polarization puzzle for S -wave charmonia [26] and bottomonia [27, 28] and the production puzzle for η_c mesons [29] have been successfully solved. Further on, a good description of the χ_{c1} and χ_{c2} production cross sections including their relative rates $\sigma(\chi_{c2})/\sigma(\chi_{c1})$ has been achieved and the corresponding LDMEs for χ_{cJ} mesons have been determined [26].

The main goal of our present note is to extend the approach [25] to the first and very new CMS data [1] on χ_{cJ} polarization. We propose a method to implement these data into the LDMEs fit procedure, thus refining the previously extracted LDMEs for χ_{cJ} mesons. Our study sheds light on the role of CO contributions which were unnecessary or even unwanted [12] for χ_{cJ} p_T spectra or their relative rates $\sigma(\chi_{c2})/\sigma(\chi_{c1})$, but which reveal now in the measured polar anisotropies. To preserve the consistency with our previous studies [26–29], we follow mostly the same steps and employ the k_T -factorization QCD

approach [30, 31] to produce the $c\bar{c}$ pair in the hard parton scattering. The newly added calculations are only for the feeddown contributions from ψ' radiative decays.

For the reader's convenience, we briefly recall the calculation details. Our consideration is based on the off-shell gluon-gluon fusion subprocess that represents the true leading order (LO) in QCD:

$$g^*(k_1) + g^*(k_2) \rightarrow c\bar{c} \left[{}^3P_J^{[1]}, {}^3S_1^{[8]} \right] (p) \quad (1)$$

for χ_{cJ} mesons with $J = 0, 1, 2$. The four-momenta of all particles are indicated in the parentheses and the possible intermediate states of the $c\bar{c}$ pair are listed in the brackets. The initial off-shell gluons have non-zero transverse momenta $k_{1T}^2 = -\mathbf{k}_{1T}^2 \neq 0$, $k_{2T}^2 = -\mathbf{k}_{2T}^2 \neq 0$ and, consequently, an admixture of longitudinal component in the polarization vectors. According to the k_T -factorization prescription [31], the gluon spin density matrix is taken in the form

$$\sum \epsilon^\mu \epsilon^{*\nu} = \frac{\mathbf{k}_T^\mu \mathbf{k}_T^\nu}{\mathbf{k}_T^2}, \quad (2)$$

where \mathbf{k}_T is the component of the gluon momentum perpendicular to the beam axis. In the collinear limit, where $\mathbf{k}_T^2 \rightarrow 0$, this expression converges to the ordinary $-g^{\mu\nu}$ after averaging over the gluon azimuthal angle. In all other respects, we follow the standard QCD Feynman rules. The hard production amplitudes contain spin and color projection operators [32] that guarantee the proper quantum numbers of the state under consideration. The respective cross section

$$\begin{aligned} \sigma(pp \rightarrow \chi_{cJ} + X) &= \int \frac{2\pi}{x_1 x_2 s F} f_g(x_1, \mathbf{k}_{1T}^2, \mu^2) f_g(x_2, \mathbf{k}_{2T}^2, \mu^2) \times \\ &\times |\bar{\mathcal{A}}(g^* + g^* \rightarrow \chi_{cJ})|^2 d\mathbf{k}_{1T}^2 d\mathbf{k}_{2T}^2 dy \frac{d\phi_1}{2\pi} \frac{d\phi_2}{2\pi}, \end{aligned} \quad (3)$$

where ϕ_1 and ϕ_2 are the azimuthal angles of incoming off-shell gluons carrying the longitudinal momentum fractions x_1 and x_2 , y is the rapidity of produced χ_{cJ} mesons, F is the off-shell flux factor [34] and $f_g(x, \mathbf{k}_T^2, \mu^2)$ is the transverse momentum dependent (TMD, or unintegrated) gluon density function. More details can be found in our previous papers [26–29]. Presently, all of the above formalism is implemented into the newly developed Monte-Carlo event generator PEGASUS [33].

As usual, we have tried several sets of TMD gluon densities in a proton. Three of them, namely, A0 [35], JH'2013 set 1 and JH'2013 set 2 [36] have been obtained from Catani-Ciafaloni-Fiorani-Marchesini (CCFM) evolution equation [37], where the input parametrizations (used as boundary conditions) have been fitted to the proton structure function $F_2(x, Q^2)$. Besides that, we have tested a TMD gluon distribution obtained within the Kimber-Martin-Ryskin (KMR) prescription [38, 39], which provides a method to construct the TMD parton densities from conventional (collinear) ones¹. Following [41], we set the meson masses to $m(\chi_{c1}) = 3.51$ GeV, $m(\chi_{c2}) = 3.56$ GeV, $m(J/\psi) = 3.096$ GeV and branching fractions $B(\chi_{c1} \rightarrow J/\psi\gamma) = 33.9\%$, $B(\chi_{c2} \rightarrow J/\psi\gamma) = 19.2\%$ and $B(J/\psi \rightarrow \mu^+\mu^-) = 5.961\%$ everywhere in the calculations below. When evaluating the feeddown contributions from ψ' radiative decays, $\psi' \rightarrow \chi_{cJ} + \gamma$, we set $m(\psi') = 3.69$ GeV, $B(\psi' \rightarrow \chi_{c1}\gamma) = 9.75\%$

¹For the input, we have used LO MMHT'2014 set [40].

and $B(\psi' \rightarrow \chi_{c2}\gamma) = 9.52\%$. The parton level calculations have been performed using the Monte-Carlo generator PEGASUS.

As it was mentioned above, to determine the LDMEs of χ_{cJ} mesons a global fit to the χ_{cJ} production data at the LHC was performed [26]. The data on the χ_{c1} and χ_{c2} transverse momentum distributions provided by ATLAS Collaboration [42] at $\sqrt{s} = 7$ TeV and the production rates $\sigma(\chi_{c2})/\sigma(\chi_{c1})$ reported by CMS [43], ATLAS [42] and LHCb [44, 45] Collaborations were included in the fit. Here we extend our previous consideration and incorporate it with the first data [1] on the χ_{c1} and χ_{c2} polarization collected by CMS Collaboration at $\sqrt{s} = 8$ TeV. In the original CMS analysis, the χ_{cJ} polarization was extracted from the (di)muon angular distributions in the helicity frame of the daughter J/ψ meson. The latter is parametrized as

$$\frac{d\sigma}{d\cos\theta^* d\phi^*} \sim \frac{1}{3 + \lambda_\theta} (1 + \lambda_\theta \cos^2\theta^* + \lambda_\phi \sin^2\theta^* \cos 2\phi^* + \lambda_{\theta\phi} \sin 2\theta^* \cos \phi^*), \quad (4)$$

where θ^* and ϕ^* are the positive muon polar and azimuthal angles, so that the χ_{cJ} angular momentum is encoded in the polarization parameters λ_θ , λ_ϕ and $\lambda_{\theta\phi}$. The ratio of the yields $\sigma(\chi_{c2})/\sigma(\chi_{c1})$ has been measured as a function of $\cos\theta^*$ and ϕ^* in three different regions of J/ψ transverse momentum, $8 < p_T < 12$ GeV, $12 < p_T < 18$ GeV and $18 < p_T < 30$ GeV, thus leading to a simple correlation between the $\lambda_\theta^{\chi_{c1}}$ and $\lambda_\theta^{\chi_{c2}}$ parameters:

$$\lambda_\theta^{\chi_{c2}} = (-0.94 + 0.90\lambda_\theta^{\chi_{c1}}) \pm (0.51 + 0.05\lambda_\theta^{\chi_{c1}}), \quad 8 < p_T < 12 \text{ GeV}, \quad (5)$$

$$\lambda_\theta^{\chi_{c2}} = (-0.76 + 0.80\lambda_\theta^{\chi_{c1}}) \pm (0.26 + 0.05\lambda_\theta^{\chi_{c1}}), \quad 12 < p_T < 18 \text{ GeV}, \quad (6)$$

$$\lambda_\theta^{\chi_{c2}} = (-0.78 + 0.77\lambda_\theta^{\chi_{c1}}) \pm (0.26 + 0.06\lambda_\theta^{\chi_{c1}}), \quad 18 < p_T < 30 \text{ GeV}. \quad (7)$$

Our main idea is to extract the LDME for ${}^3S_1^{[8]}$ contributions, $\mathcal{O}^{\chi_{c0}}[{}^3S_1^{[8]}]$, from the polarization data, since it can only be poorly determined from the measured χ_{cJ} transverse momentum distributions. To be precise, a good description of the latter can be achieved for a widely ranging $\mathcal{O}^{\chi_{c0}}[{}^3S_1^{[8]}]$, always with reasonably good $\chi^2/d.o.f.$ (see, for example, [11–13]). Moreover, its zero value is even preferable for the production rate ratio $\sigma(\chi_{c2})/\sigma(\chi_{c1})$ [12]. However, the reported production rates plotted as functions of $\cos\theta^*$ and ϕ^* have free (indefinite) normalization [46] and thus it is difficult to immediately implement them into the LDMEs fitting procedure. Therefore, we had to use the parametrizations (5) — (7) for our purposes.

Our fitting procedure is the following. First, we performed a fit of the χ_{c1} and χ_{c2} transverse momentum distributions and their relative production rates $\sigma(\chi_{c2})/\sigma(\chi_{c1})$ and determined the values of CS wave functions of χ_{cJ} mesons at the origin, $|\mathcal{R}'^{\chi_{c1}}(0)|^2$ and $|\mathcal{R}'^{\chi_{c2}}(0)|^2$, for a (large) number of fixed guessed $\mathcal{O}^{\chi_{c0}}[{}^3S_1^{[8]}]$ values in the range $10^{-4} < \mathcal{O}^{\chi_{c0}}[{}^3S_1^{[8]}] < 10^{-3} \text{ GeV}^3$. At this step we employ the fitting algorithm implemented in the GNUPLOT package [47]. Following [48], we considered the CS wave functions as independent (not necessarily identical) free parameters. The reason for such a suggestion is that treating the charmed quarks in the potential models as spinless particles could be an oversimplification, and radiative corrections to the CS wave functions could be large [48] and spin dependent. Then, we collected the simulated events in the kinematical region defined by the CMS measurement [1] and generated the decay muon angular distributions according to the

production and decay matrix elements. By applying a three-parametric fit based on (4), we determined the polarization parameters $\lambda_\theta^{\chi_{c1}}$ and $\lambda_\theta^{\chi_{c2}}$ as functions of $\mathcal{O}^{\chi_{c0}}[{}^3S_1^{[8]}]$ (see Fig. 1). We find that the dependence of these parameters on $\mathcal{O}^{\chi_{c0}}[{}^3S_1^{[8]}]$ is essential and therefore can be used to extract the latter from the data. One can see that χ_{c1} and χ_{c2} mesons have significantly different polar anisotropies, $\lambda_\theta^{\chi_{c1}} > 0$ and $\lambda_\theta^{\chi_{c2}} < 0$, which smoothly decrease when $\mathcal{O}^{\chi_{c0}}[{}^3S_1^{[8]}]$ grows². It is important to remind that each of the considered $\mathcal{O}^{\chi_{c0}}[{}^3S_1^{[8]}]$ values provides already a good fit to the p_T spectra: each value of $\mathcal{O}^{\chi_{c0}}[{}^3S_1^{[8]}]$ is associated with a respective set of commonly fitted color-singlet LDMEs. Now, using the relations (5) — (7) between $\lambda_\theta^{\chi_{c1}}$ and $\lambda_\theta^{\chi_{c2}}$ (shown by dashed curves in Fig. 1) one can easily extract $\mathcal{O}^{\chi_{c0}}[{}^3S_1^{[8]}]$ for each of the three p_T regions. Finally, the mean-square average is taken as the fitted value. Thus, this provides us with a complementary way to determine the LDMEs for χ_{cJ} mesons from the polarization data.

It is interesting to note that the determined values of $\mathcal{O}^{\chi_{c0}}[{}^3S_1^{[8]}]$ almost do not depend on the exact polarization of ${}^3S_1^{[8]}$ contributions in the CO channel. This can be easily understood because χ_{c1} and χ_{c2} mesons from the ${}^3S_1^{[8]}$ intermediate state produce very close J/ψ polarization, while the measured polar asymmetry is driven by the difference $\lambda_\theta^{\chi_{c1}} - \lambda_\theta^{\chi_{c2}}$. To illustrate it, we have repeated the calculations treating the ${}^3S_1^{[8]}$ contributions as unpolarized (yellow curves in Fig. 1). As one can see, the correlations (5) — (7) obtained in this toy approximation practically coincide with exact calculations.

The mean-square average of the extracted $\mathcal{O}^{\chi_{c0}}[{}^3S_1^{[8]}]$ values and the corresponding CS wave functions at the origin $|\mathcal{R}'^{\chi_{c1}}(0)|^2$ and $|\mathcal{R}'^{\chi_{c2}}(0)|^2$ are shown in Table 1 for all tested TMD gluon densities. The relevant uncertainties are estimated in the conventional way using Student's t-distribution at the confidence level $P = 95\%$. For comparison, we also present the LDMEs obtained in the NLO NRQCD by other authors [12, 13]. Our fit shows unequal values for the χ_{c1} and χ_{c2} wave functions with the ratio $|\mathcal{R}'^{\chi_{c1}}(0)|^2/|\mathcal{R}'^{\chi_{c2}}(0)|^2 \sim 4$ for CCFM-evolved TMD gluon densities and about of $|\mathcal{R}'^{\chi_{c1}}(0)|^2/|\mathcal{R}'^{\chi_{c2}}(0)|^2 \sim 3$ for KMR one. Thus, we interpret the available LHC data as supporting their unequal values, that qualitatively agrees with the previous results [26, 48]. This leads to a different role of CO contributions to the χ_{c1} and χ_{c2} production cross sections. So, the χ_{c1} production is dominated by the CS contributions, whereas CO terms are more important for χ_{c2} mesons (see Fig. 2).

All the LHC data involved in the fits are compared with our predictions in Figs. 2 — 4. The green shaded bands represent the theoretical uncertainties of our calculations (responding to JH'2013 set 2 gluon density), which include both the scale uncertainties and the ones coming from the LDMEs fitting procedure. To estimate the scale uncertainties, the standard variations in the scale (by a factor of 2) were applied through replacing the JH'2013 set 2 gluon density with JH'2013 set 2+, or with JH'2013 set 2-, respectively. This was done to preserve the intrinsic correspondence between the TMD set and scale used in the evolution equation (see [36] for more information). We have achieved quite a nice agreement between our calculations and available LHC data. In particular, we obtained a simultaneous description of the transverse momentum distributions and the relative production rates $\sigma(\chi_{c2})/\sigma(\chi_{c1})$. There are some deviations from the data at low p_T region, where, however,

²The influence of CO contributions on the χ_{cJ} polarization in the collinear scheme has been investigated in [49].

Table 1: The fitted values of LDMEs and CS wave functions at the origin for χ_{cJ} mesons. The results obtained in the NLO NRQCD fits [12, 13] are shown for comparison.

Source	$ \mathcal{R}'^{\chi_{c1}}(0) ^2/\text{GeV}^5$	$ \mathcal{R}'^{\chi_{c2}}(0) ^2/\text{GeV}^5$	$\mathcal{O}^{\chi_{c0}}[{}^3S_1^{[8]}]/\text{GeV}^3$
A0	0.14 ± 0.03	0.0346 ± 0.0010	$(7.0 \pm 2.0) \cdot 10^{-4}$
JH'2013 set 1	0.17 ± 0.03	0.043 ± 0.004	$(7.0 \pm 2.0) \cdot 10^{-4}$
JH'2013 set 2	0.20 ± 0.04	0.0500 ± 0.0007	$(8.0 \pm 2.0) \cdot 10^{-4}$
KMR (MMHT'2014)	0.08 ± 0.02	0.026 ± 0.002	$(4.0 \pm 1.0) \cdot 10^{-4}$
NLO NRQCD fit [12]	0.35	0.35	$4.4 \cdot 10^{-4}$
NLO NRQCD fit [13]	0.075	0.075	$2.01 \cdot 10^{-3}$

an accurate treatment of large logarithms $\ln m(\chi_{cJ})/p_T$ and other nonperturbative effects is needed.

The $\lambda_\theta^{\chi_{c2}}$ values extracted according to (5) — (7) when $\lambda_\theta^{\chi_{c1}}$ is fixed to our predictions are shown on Fig. 5. As one can see, our fit well agrees with the experimentally determined correlations between $\lambda_\theta^{\chi_{c1}}$ and $\lambda_\theta^{\chi_{c2}}$. The predicted $\lambda_\theta^{\chi_{cJ}}$ values are practically independent on the TMD gluon density and are close to the reported NLO NRQCD results [1].

To conclude, we have considered first LHC data on χ_{c1} and χ_{c2} polarizations reported very recently by the CMS Collaboration at $\sqrt{s} = 8$ TeV. We have demonstrated that the polar anisotropy of χ_{c1} and χ_{c2} mesons is strongly sensitive to the color octet contributions and proposed a method to extract the corresponding LDMEs from the polarization data. First time with the k_T -factorization approach, we have determined the color octet LDMEs and the color singlet wave functions at the origin $|\mathcal{R}'^{\chi_{c1}}(0)|^2$ and $|\mathcal{R}'^{\chi_{c2}}(0)|^2$, thus refining our previous results based on the measured χ_{cJ} transverse momentum distributions only. Our fit points to unequal color singlet wave functions of χ_{c1} and χ_{c2} states with $|\mathcal{R}'^{\chi_{c1}}(0)|^2/|\mathcal{R}'^{\chi_{c2}}(0)|^2 \sim 3$ or 4. We achieved a good simultaneous description of all available data on χ_{cJ} production at the LHC, including their transverse momentum distributions, relative production rates and polarization observables.

Acknowledgements. The authors thank H. Jung for useful discussions on the topic. We are grateful to DESY Directorate for the support in the framework of Cooperation Agreement between MSU and DESY on phenomenology of the LHC processes and TMD parton densities.

References

- [1] CMS Collaboration, arXiv:1912.07706 [hep-ex].
- [2] CMS Collaboration, Phys. Lett. B **727**, 381 (2013).
- [3] CMS Collaboration, Phys. Rev. Lett. **110**, 081802 (2013).
- [4] G. Bodwin, E. Braaten, G. Lepage, Phys. Rev. D **51**, 1125 (1995).
- [5] P. Cho, A.K. Leibovich, Phys. Rev. D **53**, 150 (1996); Phys. Rev. D **53**, 6203 (1996).
- [6] B. Gong, X.Q. Li, J.-X. Wang, Phys. Lett. B **673**, 197 (2009).
- [7] Y.-Q. Ma, K. Wang, K.-T. Chao, Phys. Rev. Lett. **106**, 042002 (2011).
- [8] M. Butenschön, B.A. Kniehl, Phys. Rev. Lett. **108**, 172002 (2012).
- [9] K.-T. Chao, Y.-Q. Ma, H.-S. Shao, K. Wang, Y.-J. Zhang, Phys. Rev. Lett. **108**, 242004 (2012).
- [10] B. Gong, L.-P. Wan, J.-X. Wang, H.-F. Zhang, Phys. Rev. Lett. **110**, 042002 (2013).
- [11] Y.-Q. Ma, K. Wang, K.-T. Chao, H.-F. Zhang, Phys. Rev. D **83**, 111503 (2011).
- [12] A.K. Likhoded, A.V. Luchinsky, S.V. Poslavsky, Phys. Rev. D **90**, 074021 (2014).
- [13] H.-F. Zhang, L. Yu, S.-X. Zhang, L. Jia, Phys. Rev. D **93**, 054033 (2016).
- [14] B. Gong, J.-X. Wang, H.-F. Zhang, Phys. Rev. D **83**, 114021 (2011).
- [15] K. Wang, Y.-Q. Ma, K.-T. Chao, Phys. Rev. D **85**, 114003 (2012).
- [16] B. Gong, L.-P. Wan, J.-X. Wang, H.-F. Zhang, Phys. Rev. Lett. **112**, 032001 (2014).
- [17] Y. Feng, B. Gong, L.-P. Wan, J.-X. Wang, H.-F. Zhang, Chin. Phys. C **39**, 123102 (2015).
- [18] H. Han, Y.-Q. Ma, C. Meng, H.-S. Shao, Y.-J. Zhang, K.-T. Chao, Phys. Rev. D **94**, 014028 (2016).
- [19] J.-P. Lansberg, H.-S. Shao, H.-F. Zhang, Phys. Lett. B **786** 342 (2018).
- [20] Y. Feng, J. He, J.-P. Lansberg, H.-S. Shao, A. Usachov, H.-F. Zhang, Nucl.Phys. B **945**, 114662 (2019).
- [21] J.-P. Lansberg, arXiv:1903.09185 [hep-ph].
- [22] LHCb Collaboration, Eur. Phys. J. C **75**, 311 (2015).
- [23] H.-F. Zhang, Z. Sun, W.-L. Sang, R. Li, Phys. Rev. Lett. **114**, 092006 (2015).
- [24] M. Butenschön, Z. G. He, B.A. Kniehl, Phys. Rev. Lett. **114**, 092004 (2015).

- [25] S.P. Baranov, Phys. Rev. D **93**, 054037 (2016).
- [26] S.P. Baranov, A.V. Lipatov, Phys. Rev. D **100**, 114021 (2019).
- [27] N.A. Abdulov, A.V. Lipatov, Eur. Phys. J. C **79**, 830 (2019).
- [28] N.A. Abdulov, A.V. Lipatov, arXiv:2003.06201 [hep-ph].
- [29] S.P. Baranov, A.V. Lipatov, Eur. Phys. J. C **79**, 621 (2019).
- [30] S. Catani, M. Ciafaloni, F. Hautmann, Nucl. Phys. B **366**, 135 (1991);
J.C. Collins, R.K. Ellis, Nucl. Phys. B **360**, 3 (1991).
- [31] L.V. Gribov, E.M. Levin, M.G. Ryskin, Phys. Rep. **100**, 1 (1983);
E.M. Levin, M.G. Ryskin, Yu.M. Shabelsky, A.G. Shuvaev, Sov. J. Nucl. Phys. **53**, 657 (1991).
- [32] C.-H. Chang, Nucl. Phys. B **172**, 425 (1980);
E.L. Berger, D.L. Jones, Phys. Rev. D **23**, 1521 (1981);
R. Baier, R. Rückl, Phys. Lett. B **102**, 364 (1981);
S.S. Gershtein, A.K. Likhoded, S.R. Slabospitsky, Sov. J. Nucl. Phys. **34**, 128 (1981).
- [33] A.V. Lipatov, S.P. Baranov, M.A. Malyshev, arXiv:1912.04204 [hep-ph];
<https://theory.sinp.msu.ru/doku.php/pegasus/news>
- [34] E. Bycling, K. Kajantie, Particle Kinematics, John Wiley and Sons (1973).
- [35] H. Jung, arXiv:hep-ph/0411287.
- [36] F. Hautmann, H. Jung, Nucl. Phys. B **883**, 1 (2014).
- [37] M. Ciafaloni, Nucl. Phys. B **296**, 49 (1988);
S. Catani, F. Fiorani, G. Marchesini, Phys. Lett. B **234**, 339 (1990);
S. Catani, F. Fiorani, G. Marchesini, Nucl. Phys. B **336**, 18 (1990);
G. Marchesini, Nucl. Phys. B **445**, 49 (1995).
- [38] M.A. Kimber, A.D. Martin, M.G. Ryskin, Phys. Rev. D **63**, 114027 (2001);
A.D. Martin, M.G. Ryskin, G. Watt, Eur. Phys. J. C **31**, 73 (2003).
- [39] A.D. Martin, M.G. Ryskin, G. Watt, Eur. Phys. J. C **66**, 163 (2010).
- [40] L.A. Harland-Lang, A.D. Martin, P. Motylinski, R.S. Thorne, Eur. Phys. J. C **75**, 204 (2015).
- [41] PDG Collaboration, Phys. Rev. D **98**, 030001 (2018).
- [42] ATLAS Collaboration, JHEP **07**, 154 (2014).
- [43] CMS Collaboration, Eur. Phys. J. C **72**, 2251 (2012).
- [44] LHCb Collaboration, Phys. Lett. B **714**, 215 (2012).

- [45] LHCb Collaboration, JHEP **10**, 115 (2013).
- [46] C. Lourenco, P. Faccioli, private communications.
- [47] www.gnuplot.info
- [48] S.P. Baranov, Phys. Rev. D **83**, 034035 (2011).
- [49] B.A. Kniehl, G. Kramer, C.P. Palisoc, Phys. Rev. D **68**, 114002 (2003).

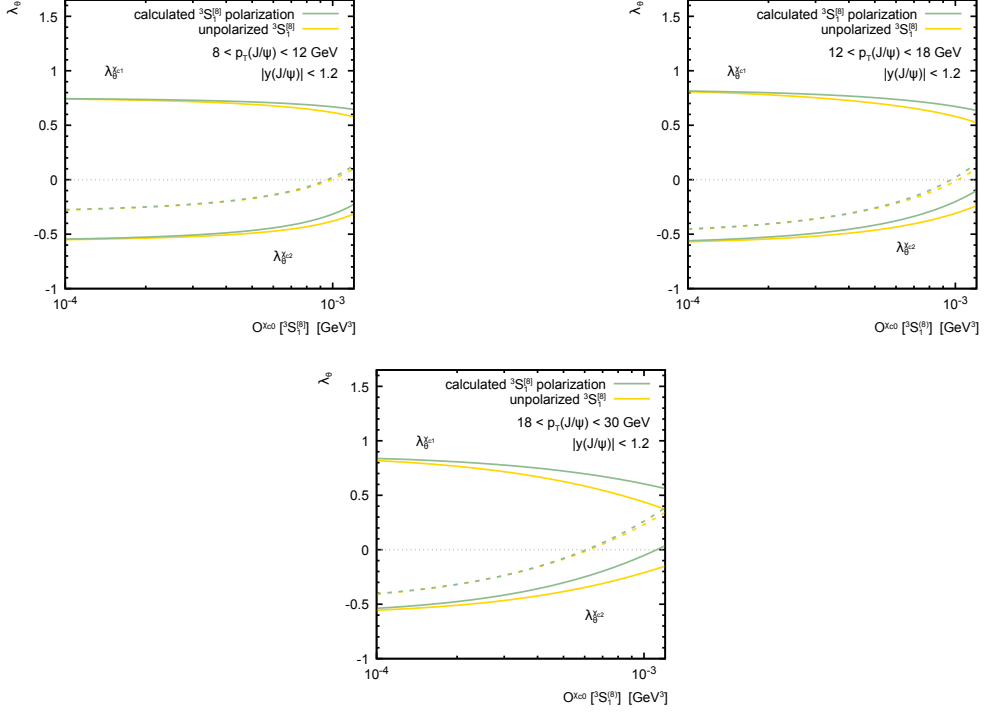


Figure 1: Polarization parameters λ_θ^{Xc1} and λ_θ^{Xc2} calculated as a functions of $\mathcal{O}^{Xc0} [^3S_1^{[8]}]$ in the helicity frame at $|y(J/\psi)| < 1.2$ and $\sqrt{s} = 8 \text{ TeV}$ in three different p_T regions. Solid green and yellow curves represent the results of exact and approximated (when the intermediate $^3S_1^{[8]}$ state is taken unpolarized) calculations. Dashed curves correspond to the correlations (5) — (7) reported by the CMS Collaboration [1]. Everywhere, the JH’2013 set 2 gluon density is used.

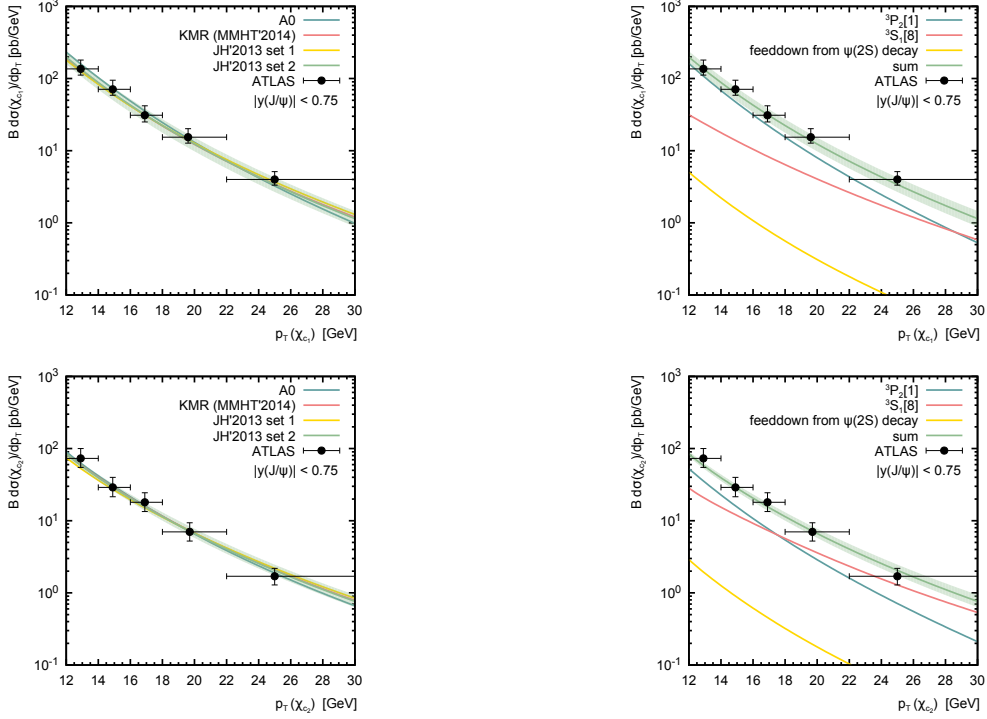


Figure 2: The prompt χ_{c1} and χ_{c2} production cross sections in pp collisions at $\sqrt{s} = 7$ TeV as a function of their transverse momenta. On left panels, the predictions obtained with different TMD gluon densities in a proton are presented. On right panels, the contributions from direct ${}^3P_J^{[1]}$, ${}^3S_1^{[8]}$ and feeddown production mechanisms are shown separately (the JH'2013 set 2 gluon distribution was used for illustration). The experimental data are from ATLAS [42].

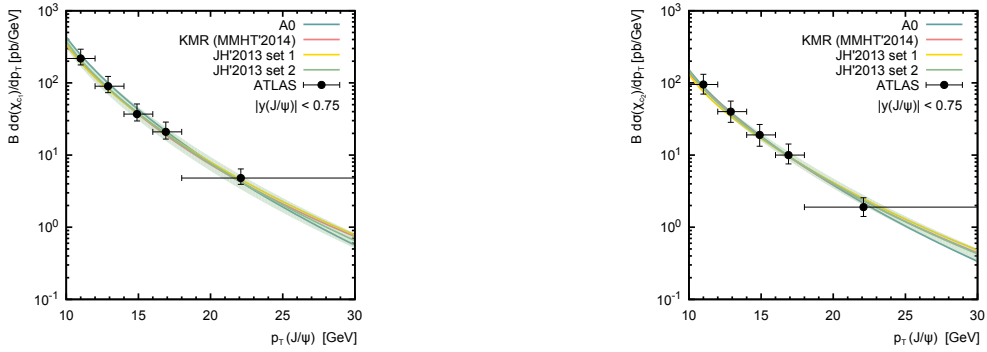


Figure 3: The prompt χ_{c1} and χ_{c2} production cross sections in pp collisions at $\sqrt{s} = 7$ TeV as a function of decay J/ψ transverse momenta. Notation of all curves is the same as in Fig. 2. The experimental data are from ATLAS [42].

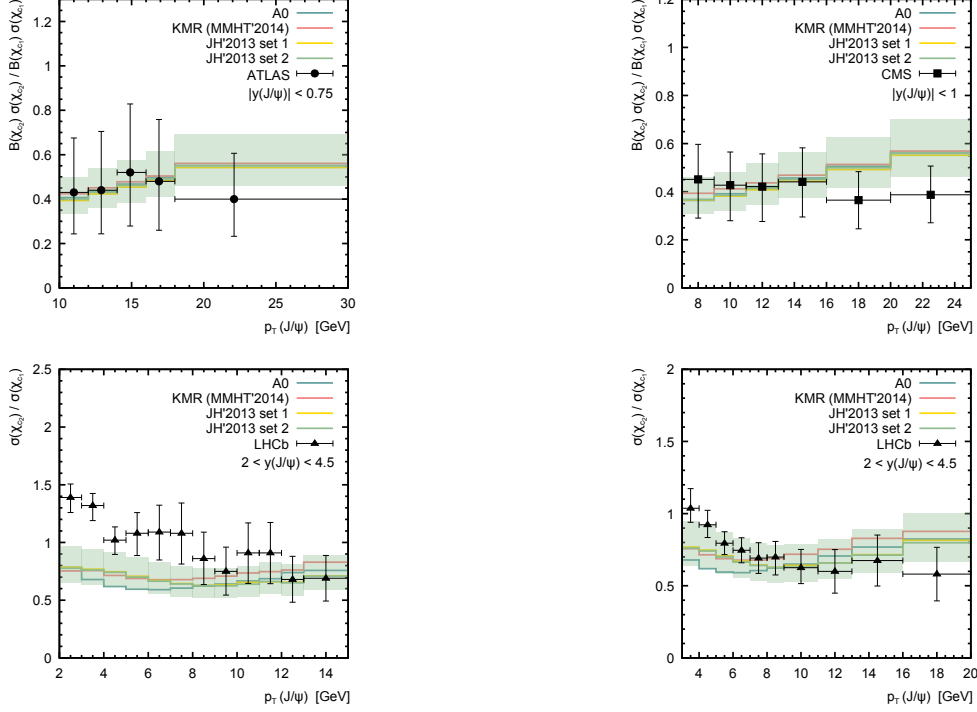


Figure 4: The relative production rate $\sigma(\chi_{c2})/\sigma(\chi_{c1})$ calculated as a function of decay J/ψ transverse momentum at $\sqrt{s} = 7$ TeV. Notation of all curves is the same as in Fig. 2. The experimental data are from ATLAS [42], CMS [43] and LHCb [44, 45].

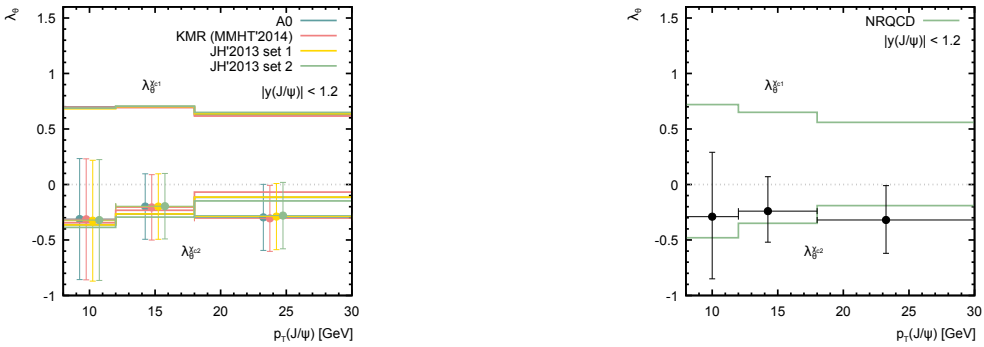


Figure 5: The $\lambda_\theta^{\chi_{c2}}$ values determined according to correlations (5) — (7) when the $\lambda_\theta^{\chi_{c1}}$ is fixed to our predictions (left panel) or NRQCD ones (right panel). The NRQCD predictions are taken from CMS paper [1].